

Magnetic counterforce for insertion devices

Roger Carr

Stanford Synchrotron Radiation Laboratory, Stanford Linear Accelerator Center, Stanford, CA, USA.

E-mail: carr@slac.stanford.edu

In a standard insertion device, such as a wiggler or undulator, the force between two rows of magnets increases exponentially as the gap between the rows decreases. This force is usually managed by a powerful mechanical gap adjustor, sometimes with the aid of springs at small values of gap. This paper is a description of how the magnetic forces can be nulled using auxiliary counterforce magnets.

Keywords: wigglers; undulators; insertion devices; magnets.

1. Introduction

The common Halbach insertion devices on storage rings that are used to create synchrotron radiation consist of rows of magnets held apart by a mechanical gap-adjustor mechanism. This adjustor must often be capable of managing several tons of force, while moving the rows of magnets parallel to each other with a precision of a few micrometers. There are issues of cost, complexity, precise control and safety involved with the management of these very large forces. In some systems, at the smallest gap setting, springs are used to counteract the force, which reduces the extreme load on the mechanism. However, no simple spring system provides the same force curve as the magnets do over a reasonable range of motion. The alternative we propose here is the use of counterforce magnets.

Consider the system shown schematically in Fig. 1. When the jaws move symmetrically, the gap between the two moving jaws closes twice as rapidly as the gap between the counterforce magnets. The main magnets attract each other, but the counterforce magnets are

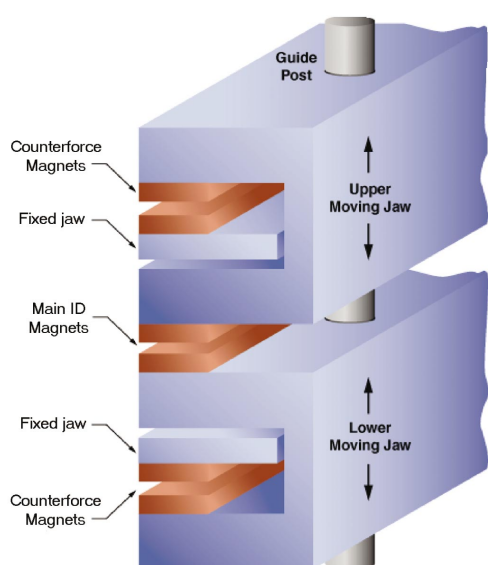


Figure 1

A schematic end view of an insertion device, showing two moving jaws with main insertion device (ID) magnets and counterforce magnets mounted on them. There are also two fixed rows of counterforce magnets opposite each set of moving magnets.

phased to repel each other. It is assumed that there is negligible interaction between the main and counterforce magnets. We will consider the case of a pure permanent-magnet device first.

2. Pure permanent-magnet insertion devices

In a common pure permanent-magnet Halbach design undulator or wiggler there are four magnets per period. These give rise to a sinusoidal magnetic field, with a maximum amplitude given by (Halbach, 1981)

$$B_{\max} = 2B_r \exp(-\pi g/\lambda) [1 - \exp(-2\pi h/\lambda)] \sin(\pi/4)/(\pi/4), \quad (1)$$

where B_r is the remanence of the magnetic material, g is the gap between the rows, λ is the period length (four magnets) and h is the vertical height of the magnet row. The counterforce magnets we propose are also sinusoidal Halbach arrays, as in the main magnet rows.

An attractive or repulsive force per unit area between two rows of magnets is proportional to the square of the magnetic field and is given by†

$$P \text{ (kPa)} = 198.9 B_{\max}^2 \text{ (T)}. \quad (2)$$

This constant is calculated assuming a sinusoidal variation of the field, but in the following we only require the variation of force with the square of the field.

We could make the counterforce magnets out of the same materials as the main magnets, but that would be expensive, given the cost of typical NdFeB magnet materials. Since we have some freedom to use a different gap with the counterforce magnets, we propose the use of inexpensive strontium ferrite magnets [$B_r = 0.4$ T, H_{cb} (coercivity) = 3.9 kOe] to counter the forces in a pure NdFeB ($B_r = 1.2$ T) insertion device. Alnico magnets could also be used; they produce more flux ($B_r = 0.8$ T) but have lower coercivity ($H_{cb} = 2.5$ kOe), so they would tend to demagnetize in our repulsive field geometry if brought too close together. Ferrite magnets can be brought closer to each other without permanent demagnetization. By making the counterforce gap smaller than the main gap, we exploit the exponential behavior of the field and allow the use of relatively weaker counterforce magnets, up to the limit of their coercivity.

Let us assume counterforce magnets of the same transverse width as the main magnets. For the forces from the two counterforce arrays to null those in the main array, we have

$$B_r^{\text{main}} \exp(-2\pi x/\lambda_m) [1 - \exp(-2\pi h_m/\lambda_m)] = 2^{1/2} B_r^{\text{counter}} \exp[-\pi(x - \Delta)/\lambda_c] [1 - \exp(-2\pi h_c/\lambda_c)], \quad (3)$$

where the subscript m refers to the main magnets, the subscript c refers to the counterforce magnets and x refers to the motion of either jaw. We have inserted an offset, Δ , so that the zero of motion of the counterforce magnets need not be the same as that for the main magnets. The $2^{1/2}$ factor appears because there are two sets of counterforce magnets and the force goes as the square of the B field.

A solution of this equation for all values of x requires that

$$2/\lambda_m = 1/\lambda_c. \quad (4)$$

Even though the following step is not required mathematically, we lose no significant performance if we set

† The energy in a magnetic field in a volume dV is given by $W = 0.5 \int \mathbf{H} \cdot \mathbf{B} dV = 0.5 \int B^2/\mu_0 dS dl$. The resulting force is $F = dW/dl = (2\mu_0)^{-1} \int B^2 dS$, and the pressure is $P = dF/dS = \langle B \rangle^2/(2\mu_0) = B_{\max}^2/(4\mu_0)$, which is equivalent to (2) in SI units.

$$h_m/\lambda_m = h_c/\lambda_c. \quad (5)$$

With these constraints, we have the offset

$$\Delta = \lambda_m(2\pi)^{-1} \ln(B_r^{\text{main}}2^{-1/2}/B_r^{\text{counter}}). \quad (6)$$

If (4)–(6) are satisfied, the force is nulled for any value of gap and period length.

The relation between the main gap and the counterforce gap is

$$g_{\text{cf}} = g_{\text{main}}/2 - \Delta. \quad (7)$$

A limit is imposed on the minimum main gap by the condition that the counterforce magnets not become so close to each other that their repulsive fields cause demagnetization of the counterforce magnet material. To reduce this limit, the counterforce magnet width could be

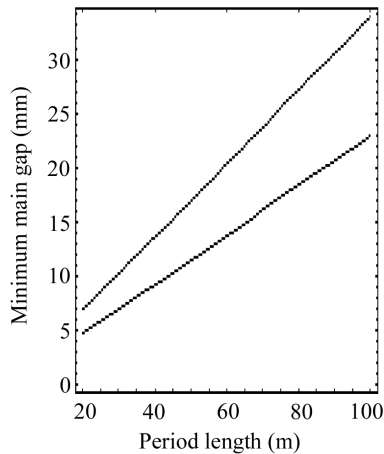


Figure 2
The minimum main gap allowed by the demagnetization of ferrite magnet material, with $B_r = 0.37$ T and $H_{\text{cb}} = 325$ kA m⁻¹. The upper curve is for the case of counterforce and main arrays of equal width, and the lower curve is for counterforce magnets twice as wide as the main magnets. Both curves assume magnets with square cross section.

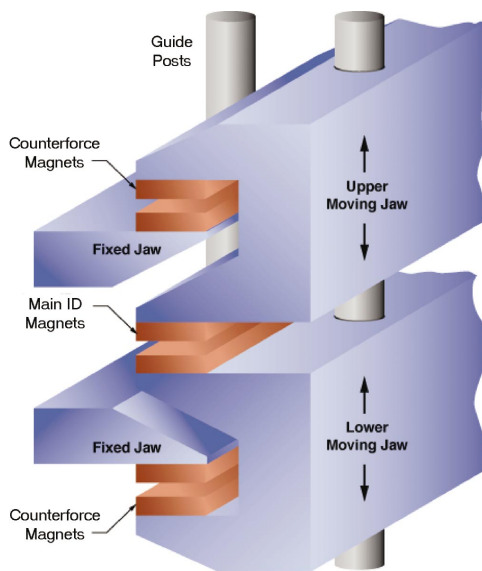


Figure 3
An alternative design, where the stationary counterforce magnets are held on a separate pillar, with supports shaped to allow more compact jaw profiles.

increased, which has the effect of decreasing the value of Δ . If r_w is the ratio of the effective width of the counterforce magnets to the effective width of the main magnets, then

$$\Delta = \lambda_m(2\pi)^{-1} \ln[B_r^{\text{main}}(2r_w)^{-1/2}/B_r^{\text{counter}}]. \quad (8)$$

An illustrative calculation is shown in Fig. 2.

Another approach would be to use counterforce magnets with higher coercivity, such as epoxy bonded NdFeB magnets, though these would be more costly than ferrite. For the main magnets we usually use an individually die-pressed and sintered grade of NdFeB. The less costly epoxy bonded material has a typical $B_r = 0.68$ T and $H_{\text{cb}} = 9$ kOe.

The essence of this approach is that one can match the attractive force of a Halbach array with counterforce from Halbach arrays. One could not achieve this balance with, say, single blocks opposed to each other.

The ‘C’ section jaws shown in Fig. 1 are only schematic; if desired for strength, the moving jaw could have a box section, with two vertical sides. There is no limit on the maximum main gap, which can be made larger by increasing the height of the moving jaws. However, the device could be made more compact, if desired, using a design like that shown in Fig. 3.

3. Hybrid insertion devices

Hybrid insertion devices are built with permanent magnets that drive flux into permeable pole pieces. The most common materials are NdFeB or SmCo for the permanent magnets and vanadium permendur for the poles. For NdFeB, the magnetic field is given by (Ellemaume *et al.* 2000)

$$B_{\text{max}}(\text{T}) = 3.694^{-g(5.08-1.52g/\lambda)/\lambda}, \quad 0.1 < g/\lambda < 1.0. \quad (9)$$

The field of a hybrid device is typically stronger than that of a pure permanent-magnet device. We could counter the forces in a hybrid device either with a permanent-magnet system or with a hybrid system. It would be preferable, on grounds of simplicity and cost, if counter-action could be accomplished with a pure permanent-magnet system. This approach would require that

$$3.694 \exp\{-2x[5.08 - 1.52(2x/\lambda_m)]/\lambda_m\} = 2^{1/2} B_r^{\text{counter}} \exp[-\pi(x - \Delta)/\lambda_c][1 - \exp(-2\pi h_c/\lambda_c)], \quad (10)$$

where the left-hand side is the field of the hybrid main magnet and the right-hand side is the field of the pure permanent counterforce magnet. There is not an exact algebraic solution for all gaps and period lengths, but approximate fits can be found. For example, with $\lambda_m = 50$ mm we obtain the fit shown in Fig. 4.

There is a coercivity limit on the counterforce gap in the hybrid case as well, which limits the minimum main gap. This limit can be extended by increasing the width of the counterforce magnets, as in the pure permanent-magnet case.

A pure permanent-magnet counterforce prototype system was built at this laboratory; a photograph is shown in Fig. 5.

The prototype has four periods of NdFeB main magnets, each 16.25 mm square by 40 mm in the transverse direction. The counterforce magnets are strontium ferrite blocks with one-quarter of this cross section and the same length transversely. The minimum main gap is 22 mm, and the minimum counterforce gap is about 2.5 mm. In the absence of the counterforce magnets, a torque of about 5.85 N m would have to be applied at the minimum gap to separate the main magnets. The torque that is actually required is about 0.3 N m; this

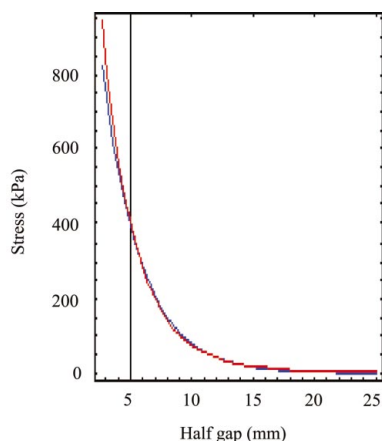


Figure 4
Stress curves for hybrid (red) and pure ferrite counterforce (blue) magnets. This fit was achieved with $\Delta = 7.7$ mm, $\lambda_c = 0.8\lambda_m$, and equally wide main and counterforce magnets.



Figure 5
A prototype counterforce system. The black jaws hold the main magnets (gold keepers in center) and the moving counterforce magnets (gold keepers at bottom and top). The red fixtures hold the stationary counterforce magnets. The lead screw is 12.7 mm in diameter with a pitch of 0.787 mm^{-1} . The crank handle is 65 mm from axis to handle axis.

value does not vary with gap and is just the constant torque required to overcome friction in the lead screw and to move the mass of the jaws against gravity. This prototype shows experimentally the predictions of the theory for the pure permanent-magnet case.

4. Discussion

We have shown how the magnetic forces in insertion devices may be nulled using simple inexpensive arrays of counterforce magnets. This technique offers the possibility of substantially reducing the cost and complexity of the gap-adjuster mechanism. Strontium ferrite ceramic magnets cost about 1% as much as NdFeB (which costs about USD 4 per cubic centimeter). The materials for an array of

$1000 \times 50 \times 100$ mm ferrite magnets would cost only about USD 200, so the mechanical structure and assembly would dominate the cost. The same volume of NdFeB main magnets would cost about USD 20000.

Gravitational forces on both the magnet jaws could also be nulled by the use of counterweights or constant-force springs. These would allow, in the absence of binding caused by unbalanced transverse forces, the use of a linear drive system of very small capacity and expense but with high speed and precision. For each jaw, the main magnets' attractions tend to rotate the jaw about its long axis in the direction opposite to the rotation caused by the counterforce magnets' repulsion. Hence, there should be no net torque, and the actuator drive could be in-line between the support pillars.

In principle, counterforce could be achieved by placing an equal but opposite magnet array on the other side of the support columns to the main magnets, on a symmetrical jaw structure. However, this would require high-performance magnets with the same period as the main magnets, and the torque about the longitudinal axis would add, causing a binding effect.

The main insertion-device magnets attract each other, so they tend to center the transverse force. The counterforce magnets repel each other and thus sit at a point of instability with respect to the transverse force. Any inaccuracy in their alignment will create transverse forces. Although these will be small for small displacements, this detail merits some attention.

In conventional insertion devices, the girders holding the magnets are supported at two points, usually the Airy points, to minimize deflection. However, when the girders are loaded by magnetic forces, they do deflect, so very rigid beams are required. Girder deflection is particularly important for long devices, because deflection increases as the cube of length. With the counterforce magnets, however, the repulsive and attractive forces cancel everywhere along the length of the moving jaw and thus null the deflection of the girder. This effect may be understood by the following argument. If there were no counterforce magnets, the beams would bow towards each other with decreasing gap. If there were no main magnets, the beams would bow away from each other with decreasing gap. With both magnet arrays in place, the tendency to bow cancels.

It is fortunate that the period of the counterforce magnets is less than that of the main magnets, because their stray fields will decay at very short distances. One should expect negligible magnetic-field perturbation at the beam axis from the counterforce magnets. The counterforce magnet arrays need to be made with little consideration for the local imperfection of their magnetic fields, as such errors will generate negligible net force imbalance.

The author is pleased to thank Allen Johnson for his useful comments about the coercivity limits on the counterforce magnets, and Ben Poling and Mike Swanson for their expert work in the design and fabrication of the prototype. This work was supported by the US Department of Energy, contract No. DE-AC03-76SF00515.

References

- Elleaume, P., Chavanne, J. & Faatz, B. (2000). *Nucl. Instrum. Methods Phys. Res. A*, **455**, 503–523.
- Halbach, K. (1981). *Nucl. Instrum. Methods Phys. Res.* **187**, 109.